

Proton and metal adsorption onto bacterial consortia: Stability constants for metal–bacterial surface complexes

Kelly J. Johnson, Jennifer E.S. Szymanowski, David Borrok¹,
Terri Q. Huynh, Jeremy B. Fein^{*}

Department of Civil Engineering and Geological Sciences, University of Notre Dame, Notre Dame, IN 46556, USA

Received 27 June 2006; received in revised form 6 December 2006; accepted 9 December 2006

Editor: D. Rickard

Abstract

In this study, we conduct potentiometric titrations and metal adsorption experiments (Cd, Ca, Cu, Pb, Sr, and Zn) using bacterial consortia grown from three representative locations and sampled over the course of a year in order to determine whether bacterial diversity affects proton and metal uptake behaviors. We observe significant changes in bacterial diversity from one site to another, and from month to month during the study period. Despite these changes in diversity, all of the bacterial consortia studied exhibit similar proton and metal uptake, strongly suggesting universal adsorption behavior for the bacterial species present in these samples. We demonstrate that a single, metal-specific, averaged surface complexation model can be used to reasonably account for the acid/base and metal adsorption behaviors of each consortium. We use a four discrete site non-electrostatic model to describe the protonation of the consortia functional groups, with averaged pK_a values of $3.2+0.2/-0.4$, $4.8+0.2/-0.3$, $6.5+0.3/-0.8$, and $9.2+0.1/-0.3$, and site concentrations of $(1.0\pm 0.28)\times 10^{-4}$, $(1.2\pm 0.23)\times 10^{-4}$, $(6.12\pm 1.1)\times 10^{-5}$, and $(9.7\pm 2.0)\times 10^{-5}$ moles of sites per gram wet mass of bacteria, respectively. The metal adsorption data are used to constrain site-specific bacterial surface complexation models, and we determine the stability constants for the important metal–bacterial surface complexes. These calculated stability constants correlate well to known stability constants for metal–acetate complexes, yielding predictive relationships that enable the estimation of the extent of adsorption of other metals onto bacterial consortia. This study demonstrates that a wide range of bacteria exhibit similar proton and metal adsorption behaviors, and that a single set of averaged acidity constants, site concentrations, and stability constants for metal–bacterial surface complexes can be used to model the adsorption behavior.

© 2006 Elsevier B.V. All rights reserved.

Keywords: Consortia; Adsorption; Bacteria; Metal; Surface complexation

1. Introduction

Bacterial surfaces can adsorb a wide range of heavy metal contaminants (e.g., Beveridge and Murray, 1976; Beveridge and Koval, 1981; Mullen et al, 1989). To better constrain and mitigate contaminant transport in the environment, it is important to develop models that determine the influence of bacteria on the speciation and distribution of heavy metals in the sub-surface. Site-

^{*} Corresponding author. Tel.: +1 574 631 6101; fax: +1 574 631 9236.

E-mail address: fein@nd.edu (J.B. Fein).

¹ Current Address: U. S. Geological Survey, Denver Federal Center, Denver, CO 80225, USA.

specific surface complexation models, originally developed to quantify cation adsorption to mineral surfaces, have been successfully used to account for proton and metal adsorption to bacterial surfaces (e.g., Plette et al., 1996; Fein et al., 1997; Haas et al., 2001; Martinez et al., 2002). However, if each bacterial species exhibits unique adsorption characteristics as mineral surfaces do, then it would be an overwhelming task to determine the stability constants, site concentrations and acidity constants necessary for modeling metal adsorption onto all of the bacteria of environmental and geologic interest. A single location in a natural system can contain many bacterial species, and bacterial diversity can change from one location to another. Consequently, if surface complexation models are to be applied to realistic systems, it is important to determine if proton and metal adsorption behavior is species-specific or if commonalities exist among bacterial species.

A number of studies have noted similar adsorption behavior among individual bacterial species (e.g., Daughney et al., 1998; Small et al., 1999; Kulczycki et al., 2002; Ngwenya et al., 2003) and among artificial mixtures of pure strains of bacteria (Yee and Fein, 2003). Yee and Fein (2001) hypothesized that similarities in adsorption mechanisms exist for a wide range of bacterial species, and they conducted potentiometric titrations and Cd-bacteria adsorption experiments using a range of Gram-positive and Gram-negative species. Yee and Fein (2001) observed similar adsorption behavior for the variety of bacteria studied, suggesting that the structures that give rise to metal and proton adsorption are common over a wide range of bacterial species.

The hypothesis of universal bacterial adsorption behavior has been supported by a number of subsequent experimental studies. For example, Jiang et al. (2004) demonstrated that the attenuated total reflectance Fourier-transform infrared spectra of both Gram-positive and Gram-negative bacteria are similar and exhibit similar variations as a function pH. These similarities suggest a similarity in binding environments for metals between species, supporting a universal adsorption behavior that arises from similar cell wall functional group chemistries. Borrok et al. (2004a) measured H^+ and Cd adsorption onto bacterial consortia from a range of natural environments, demonstrating that the consortia exhibit similar proton and Cd adsorption behaviors, and that the adsorption onto all of the consortia can be modeled using a single set of stability constants. In addition, Borrok et al. (2005) compiled all currently available potentiometric titration datasets for individual bacterial species and bacterial consortia, noting general similarities in the proton adsorption behaviors and presenting an

internally-consistent averaged set of ‘universal’ thermodynamic proton binding and site density parameters for modeling bacterial adsorption reactions in geologic systems. Although a large number of bacterial species appear to exhibit broadly similar adsorption behavior, some studies suggest that at least some bacteria have significantly different adsorptive properties. For example, Borrok et al. (2004b) showed that some bacteria that thrive in hydrocarbon-contaminated environments exhibit significantly enhanced adsorptive behavior compared to those from uncontaminated systems.

In this study, we expand the study of natural consortia of Borrok et al. (2004a) to test whether we observe similarities in binding environments for a much wider range of bacterial species than was tested by Borrok et al. (2004a), and we measure the extent of adsorption of other metals onto bacterial consortia as well. We obtain our range of bacterial diversity by growing consortia from samples taken from three natural settings and sampling those settings over the course of a year. We conduct potentiometric titrations using these bacterial consortia, and we measure the extents of Ca, Cd, Cu, Pb, Sr, and Zn adsorption onto the consortia as well. The results suggest strong similarities in binding environments on the bacterial cell walls, and we use the measurements to determine average stability constants for the important metal–bacterial surface complexes. We use the stability constants to constrain relationships between these values and metal–acetate stability constants so that our results can be extrapolated to other metals of environmental interest.

2. Methods

2.1. Sampling and growth of bacteria

Sample locations were in northern Indiana and included a river, a forest, and a soybean field site. Samples were collected 7 times from all three sites over the course of a year (October 2004 through September 2005) for potentiometric titration and Cd adsorption experiments. River water samples were also collected from October 2005 through January 2006 for follow-up experiments involving other metal cations. Bottles and scoops used to collect samples were sterilized and sealed in plastic bags before use. Water samples were collected by dipping the sample jar directly into the river. Soil samples were collected by removing the top 5 to 10 cm of topsoil and debris, and then directly scooping the soil specimen using the glass sample jar. Lids were placed loosely over the jars to allow for aerobic conditions and to prevent contamination.

Approximately 10 mL of water from the river samples were used to inoculate 2 L of LB broth (Sambrook et al., 1989). Ten grams of soil from the forest or soybean samples were used to inoculate 75 mL of LB broth. To dilute the solid fraction present in the soil samples, approximately 10 mL of the initial bacteria–broth suspension were used to inoculate larger quantities of identical broth solutions. Samples were shaken gently at room temperature for a total of 7 days before they were harvested for experiments.

Many bacterial species are unculturable, and experiments have shown that within a natural consortium many species cannot survive repeated inoculations (Kaerberlein et al., 2002). Therefore, the bacteria grown from our experiments are likely a subset of the total bacterial population at each sample site. For example, because all growth conditions were aerobic, all anaerobes that may have been present in each environment were eliminated through the growth procedures. However, our experimental approach employing a single re-inoculation insured that the bacterial consortia produced from each sampling had a range of the bacteria that was present in each environment, but also had sufficient biomass to conduct the experiments. All experiments were conducted within seven days of sampling. We did not determine the growth phase of each bacterial species under the experimental conditions, so it is possible that not only were the consortia diverse in terms of species present, but also in terms of growth phase position of each species.

To prepare bacteria for potentiometric titrations and metal adsorption experiments, following the initial 7 day growth period, bacteria were harvested by centrifugation for 10 min at 6000 rpm (2220 g) and then rinsed 5 times with a 0.1 M NaClO₄ solution. NaClO₄ was chosen as the electrolyte because perchlorate does not bind protons or the metals of interest to an appreciable extent under the experimental conditions. After each wash, bacteria were suspended in clean electrolyte in a test tube using a vortex machine and stir rod. Bacteria were then centrifuged for 3 min at 7200 g to form a bacterial pellet, and the supernatant was decanted. Following the final wash, bacteria were resuspended in test tubes and centrifuged (7200 g at 25 °C) for 1 h, stopping 2 times to decant the supernatant. Following centrifugation, the wet weight of the bacteria was determined and used for calculation of bacterial concentrations for experiments. For a discussion on wet vs. dry weight, see Borrok et al. (2004a). The bacteria were immediately used in titrations or metal adsorption experiments. The bacterial cells remain viable after the washing treatment; however, they are not likely to be undergoing active metabolism due to the thorough wash, the lack of

nutrients and electron donors in the experimental solutions, and the relatively short (<3 h) experimental durations.

2.2. Potentiometric titrations and metal adsorption experiments

Prior to titrating bacteria, 0.1 M NaClO₄ was purged of CO₂ by N₂ bubbling for 60 min. Following this step, the harvested bacteria (0.41±0.02 g) were suspended in 12.13±0.13 mL of the electrolyte, and titrations were conducted in an N₂ atmosphere with an automatic burette assembly. When conducting titrations, the acid or base was added in minute amounts when the stability of the suspension attained a change of 0.1 mV s⁻¹ or less. The suspensions were titrated with 1.001 N HNO₃ to pH≈2.3, and then they were titrated with 1.037 N NaOH to pH≈10. We chose to titrate to the lower pH because proton adsorption onto bacterial cell walls can occur down to at least pH 2.3 (Fein et al., 2005). Potentiometric titrations were performed for all river, soybean field, and forest sample consortia grown throughout the year, and in most cases three replicate titrations were performed for each consortium.

Metal adsorption experiments were performed as a function of pH using Ca, Cd, Cu, Pb, Sr, and Zn. Cd adsorption experiments were completed for all river, soybean field, and forest sample consortia grown throughout the year. All other metal adsorption experiments were conducted using the October, 2005 through January, 2006 river samples in order to investigate linear free energy relationships that exist for metal binding onto the dominant bacterial surface sites. All experiments were conducted with freshly sampled/grown bacteria. Cd adsorption kinetics experiments were conducted for each of the types of samples at a pH between 6.0 and 6.5, and full equilibrium was reached within 1.5 h for all consortia tested.

For all Cd adsorption experiments, approximately 10 g L⁻¹ of a bacterial consortium was suspended in a pH-neutralized stock solution of 0.1 M NaClO₄ and approximately 10.3 ppm (9.2×10⁻⁵ M) Cd. In all adsorption experiments, the exact concentrations of both the bacteria and the metal of interest were determined gravimetrically. The respective bacterial concentrations for experiments involving Ca, Cu, Pb, Sr, and Zn, are: 11.4, 5.7, 3.3, 20.1, and 11.3 g L⁻¹, respectively, and their respective metal concentrations are: 5.24 (1.3×10⁻⁴ M), 5.25 (8.3×10⁻⁵ M), 10.13 (4.9×10⁻⁵ M), 3.19 (3.6×10⁻⁵ M), and 10.31 (1.6×10⁻⁴ M) ppm. These concentrations were chosen after preliminary experimentation (results not shown) to

insure that at least 30–40% of each metal was adsorbed under the highest pH conditions studied. Following a 10 min initial equilibration period, the metal/bacteria stock solution was divided into individual polypropylene reaction vessels. The pH of the suspensions in these vessels was then adjusted to the desired pH by adding minute aliquots of 0.1 to 1 M HNO₃ or NaOH. The vessels were then rotated slowly end over end on a rotating rack for 2 h, and the final pH was measured. Each reaction vessel was then centrifuged at 4500 g for 3 min, and the supernatant was collected after being filtered through a 0.45 µm filter (Osmonics Cameo 30 N). The filtered solutions were acidified with a small aliquot of concentrated HNO₃ and stored at 4 °C for no longer than 7 days prior to analysis for dissolved metal concentration. The final dissolved metal concentration in each of the sample supernatants was determined by inductively coupled plasma–optical emission spectroscopy (ICP–OES), with matrix-matched standards for calibration. The amount of metal that was adsorbed onto the bacteria during each experiment was determined as the difference between the measured concentration of metal in solution at the end of the experiment and the known initial metal concentration. Control experiments without bacteria were performed simultaneously to determine the amount of nonspecific metal adsorption onto the experimental apparatus.

2.3. Gram staining and DGGE analysis

Gram staining was performed periodically throughout the year on consortia grown from each of the 3 sample sites by heat-fixing the cells to a glass slide and then staining the cells using a PROTOCOL Gram stain kit from Fisher Scientific. DGGE analysis was performed for all consortia collected between October 2004 and September 2005 to better constrain community speciation and qualitatively assess the change in bacterial diversity throughout the year. A MoBio Laboratories, Inc. Ultraclean soil DNA kit was used to extract DNA, which was frozen at –20 °C prior to amplification. To prepare the DNA for DGGE analysis, a polymerase chain reaction (PCR) process using a custom-made universal bacterial primer set (EUB 341 and EUB 534, 200 base pairs in length with a GC-clamp) was used to amplify a specific 16s rDNA sequence (Muyzer et al., 1993). DGGE was performed using a Dcode universal mutation detection system (Bio-Rad). The PCR product DNA was loaded into a gel with a 30% to 60% gradient composed of urea and formamide (a chemical denaturant), and an electrical potential was applied to force the DNA to travel through the gel. Gels

were run at 60 °C and a potential of 60 V for 14 h. Ethidium bromide was used to stain the gel, it was then photographed using a Kodak EDAS 290 photographic system. Bacterial species have different DNA base pair sequences, therefore, the DNA for each species forms a characteristic band in the gel because it denatures at a specific point along the gel. Because the intensity of the band is directly related to the concentration of DNA in the sample, analysis of the band positions and intensities can determine the minimum number of bacterial species present and their relative abundances. The DGGE analysis sufficiently demonstrates the change in bacterial populations with sample times and locations, but additional sequencing of the bands would be required to verify that each band represents only one species and to determine the identity of the species.

3. Results and discussion

3.1. Bacterial diversity

The Gram staining results indicate that the bacterial populations of each consortium contained both Gram-negative and Gram-positive bacterial species. There was not a distinguishable trend in the relative abundances throughout the year. In each sample, there was generally a mix of rod-shaped, cocci, and spirilla bacteria, and the Gram-negative bacteria were generally 2 to 10 times smaller than the Gram-positive bacteria. The consortia grown from the river water samples were generally dominated by Gram-negative bacteria, but there were 2 months (January and May) when the bacteria had equal amounts of both, and 1 month (September) when Gram-positives were more abundant. The bacteria harvested from the forest and soy field sample sites typically contained a similar ratio of Gram-positive and Gram-negative, with a larger number of Gram-negative bacteria during the winter months (January) and more Gram-positive species toward the end of summer (September).

The consortia used in this study displayed between 6 and 14 bands (Fig. 1) in the DGGE analysis. The greatest population diversity occurred in the March consortia for all sample sites (the river and forest site consortia displayed 14 bands each, and the soy field site consortium displayed 13 bands). The lowest number of bands generally occurred during the months of November and December. Bacterial species populations typically vary from site to site and as a function of time; therefore our sampling approach was successful in creating bacterial consortia with a wide range of diversity, thereby enabling a rigorous test of adsorption behavior as a function of changing bacterial diversity.

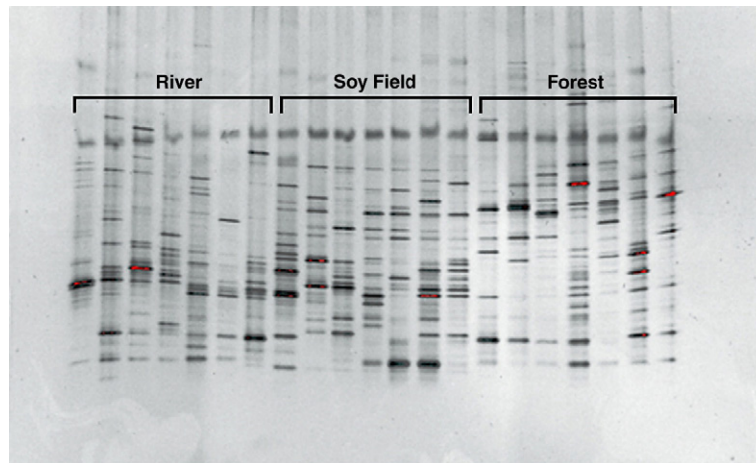


Fig. 1. DGGE gel with labeled site locations. Each section contains a lane for each sampling month, Oct., Nov/Dec., Jan., March, May, June, and September. Each band in a lane represents a different bacterial species.

3.2. Potentiometric titrations

All titration data are plotted in terms of moles of deprotonated sites per mass of bacteria,

$$\text{Net Molality Protons Added} = (C_a - C_b - [\text{H}^+] + [\text{OH}^-])/m_b \quad (1)$$

where C_a and C_b are the concentrations of acid and base added at each step of a titration, brackets represent molal species concentrations, and m_b is the bacterial wet weight suspension concentration (g L^{-1}). Fig. 2A illustrates that the titration results for the 21 consortia grown in this study are virtually identical to each other. Although there are slight differences between individual titration curves, there are no significant trends in those differences between the titration curves for the consortia from one site relative to the others, nor as a function of sampling time during the year. All consortia displayed a significant buffering capacity over the entire pH range of this study (2.5–9.5). The curves exhibited a similar shape to those exhibited by natural consortia and by a wide range of individual bacterial species (e.g., Plette et al., 1995; Fein et al., 1997; Haas et al., 2001; Yee and Fein, 2001; Martinez et al., 2002; Ngwenya et al., 2003; Borrok et al., 2004a; Fein et al., 2005). On a per gram basis, the natural consortia exhibited an average buffering capacity of $4.58 \times 10^{-4} \text{ mol g}^{-1}$ over the experimental pH range, a similar buffering capacity to the $3.0 \times 10^{-4} \text{ mol g}^{-1}$ buffering capacity exhibited by *Bacillus subtilis* over a pH range of 3–10 (Fein et al., 2005).

3.3. Metal adsorption experiments

In general, the extent of Cd adsorption to natural consortia was similar for the river, soy field, and forest sites (Fig. 3). While the river consortia in general adsorbed slightly less Cd than the others, the consortia slightly grown from the soy field and forest environments demonstrated indistinguishable adsorption capacities. There was not a noticeable trend in Cd adsorption as a function of time of sampling. These results indicate that the large changes in species diversity that are depicted in the DGGE results in Fig. 1 do not have a large impact on the Cd adsorption behaviors. The extent of Cd adsorption in this study is higher than that observed in the similar study conducted by Borrok et al. (2004a); both studies were conducted at the same ionic strength and bacterial and Cd concentrations, however Borrok et al. (2004a) used a different growth medium and they froze some consortia samples prior to experimentation. At pH 7, we observed 75 to 92% Cd adsorption and Borrok et al. (2004a) observed 52–70% metal adsorption for their natural consortia experiments; however, in their study of Cd adsorption to consortia grown from contaminated environments, Borrok et al. (2004b) reported 75–95% Cd adsorption at pH 7. In single species Cd adsorption experiments, Fein et al. (1997) observed a similar extent of Cd adsorption to the results in this study. The results of the adsorption experiments with other metals are depicted in Fig. 4. In general, the observed extents of Ca, Cu, Pb, Sr, and Zn adsorption onto the river water consortia were similar to those observed for individual bacterial species (Fein et al.,

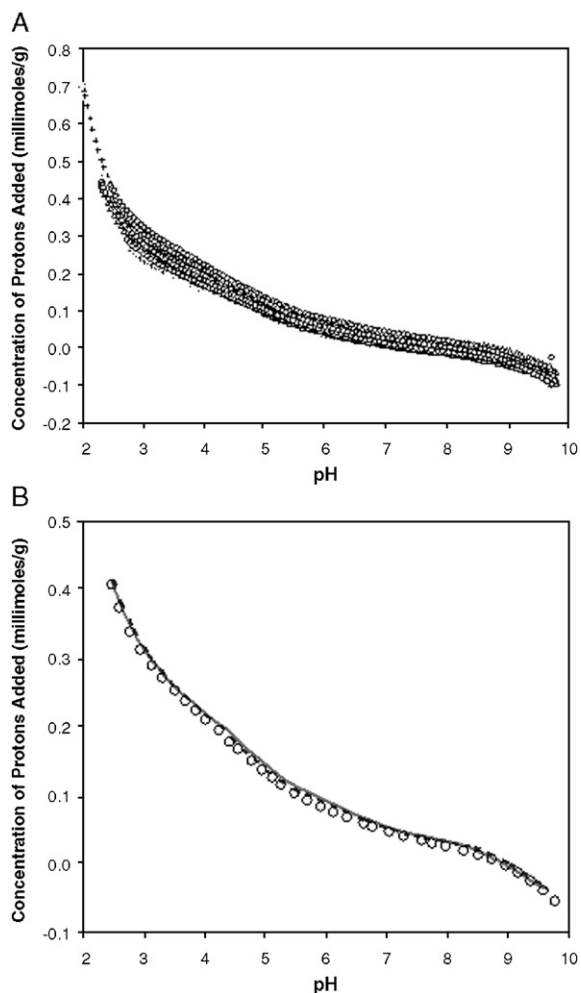


Fig. 2. (A) Potentiometric titration results for all titrations conducted for (+) river, (Δ) soybean crop, and (O) forest sites. (B) Example experimental potentiometric titration data (O) for the September soy field consortium sample. Model curves calculated using the averaged pK_a values and surface site concentrations (solid line) and the titration specific model (dashed line) are shown for comparison.

1997; Fowle and Fein, 1999; Fein et al., 2001; Borrok et al., 2005) under similar experimental conditions.

3.4. Surface complexation modeling

The diversity of the bacterial species that are represented in the natural consortia of this study did not have a large impact on the proton or Cd uptake capabilities of the consortia. This suggests that the adsorption behavior of all of the consortia can be modeled using a thermodynamic modeling approach with a single set of averaged thermodynamic parameters. Although a range of types of models can be used to account for the proton and metal adsorption behavior, we choose to apply a discrete

site, non-electrostatic surface complexation model (SCM), similar to that applied by Borrok et al. (2004a) and by Fein et al. (2005). When applying this approach to model the acidity of the surfaces of the consortia, we assume that adsorption is due to proton and metal cation interaction with negatively charged organic acid functional groups on the bacterial cell walls. This approach implicitly treats the numerous cell wall types in each consortium studied as an average cell wall with a limited number of types of functional groups. Clearly, if individual cell walls exhibit unique adsorption characteristics, it would be impossible to successfully apply this type of simplified approach. Therefore, a major objective of this modeling exercise is to determine if such an approach can successfully account for the observed adsorption behaviors.

In the discrete site modeling approach, the deprotonation of each functional group type is represented as a single deprotonation reaction (e.g., Fein et al., 1997; Ngwenya et al., 2003; Borrok et al., 2004a; Fein et al., 2005). This SCM is likely a simplification of the mechanisms involved and should not be taken as an exact representation of what is a complex and heterogeneous chemical system. In our modeling approach, the surface charge of the bacterial cell walls is due to deprotonation reactions according to the following stoichiometry:



where R represents the bacterial cell wall to which each functional group type, A_i, is attached. Mass balance

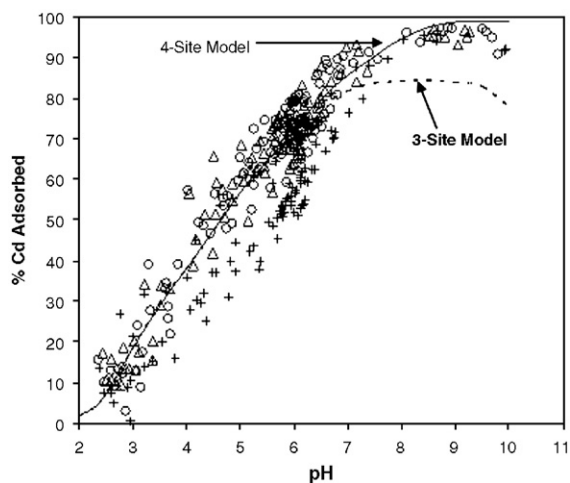


Fig. 3. Cd adsorption onto the bacterial consortia from the (+) river, (Δ) soybean crop, and (O) forest sites. Cd experiments were conducted with 10.5 ± 0.1 g bacteria/L (wet weight) and 10.31 ± 0.02 ppm (9.2×10^{-5} M) Cd in a 0.1 M NaClO₄ solution. Solid and dashed curves represent the best-fitting 4- and 3-site models, respectively, calculated using the set of averaged thermodynamic parameters (see text).

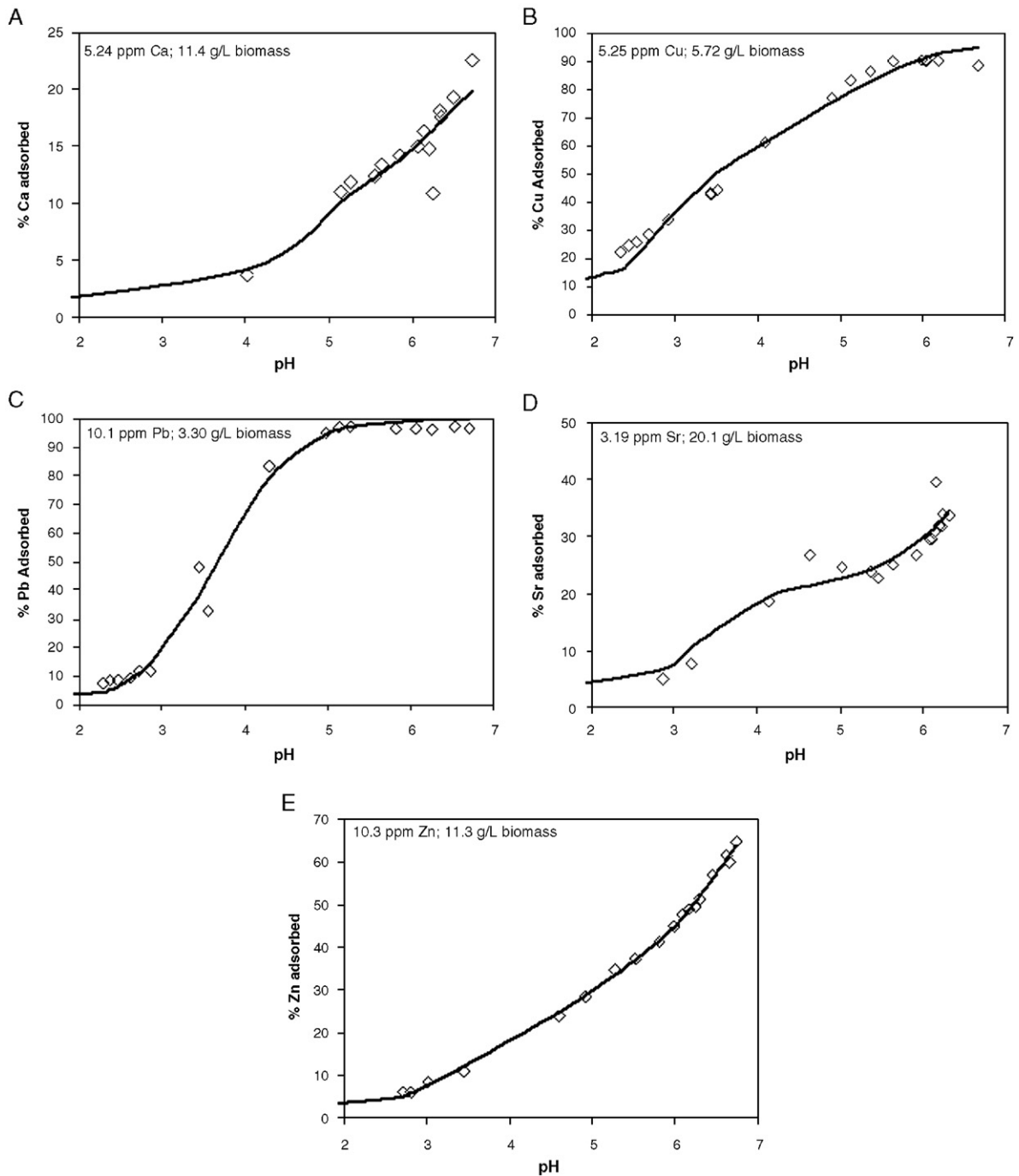


Fig. 4. Metal adsorption data for Ca, Cu, Pb, Sr, and Zn. (\diamond) = experimental data, and solid curves depict the best-fitting models.

equations are used to quantify the distribution of protonated and deprotonated functional groups, in terms of the acidity constant for Site A_i , K_a :

$$K_a = \frac{[R-A_i^-]a_{H^+}}{[R-A_iH^0]} \quad (3)$$

where $[R-A_i^-]$ and $[R-A_iH^0]$ represent the concentration of deprotonated and protonated sites, respectively, in mol/L, and a_{H^+} represents the activity of protons in the bulk solution. The data are modeled using a non-electrostatic approach because all experiments were conducted at the same ionic strength. Therefore,

potential ionic strength effects on the surface electric field could not be determined. Also, in order to apply an electrostatic model to this system, the surface area of the bacteria of interest would have to be determined. However, each consortium contained a variety of bacterial species that changed throughout the sampling period. Therefore, the overall surface area can not be calculated easily or with any certainty. Because the solvent contained protons, the same element as the one that is reacting with the surface of interest, we define a zero proton condition for the cell wall to account for the change in the proton concentrations relative to that condition (Westall et al., 1995). The same approach was used by Fein et al. (2005). The fully protonated cell wall was chosen to represent our zero proton condition, using FITEQL 2.0 (Westall, 1982) to solve for the initial protonation state of the cell walls in each titration.

The titration data were used not only to determine how many types of functional groups must be invoked in order to account for the observed buffering capacities, but also to constrain the functional group site concentrations and their associated proton binding constants (K_a). Similar to what Borrok et al. (2004a) observed for titrations of bacterial consortia, in each case a model that includes four different functional group types yields a better fit to the titration data than do models with fewer site types. In each case, a five-site model does not converge, indicating that parameters for five sites can not be constrained by the available data, and that the system is over-determined with five sites. The goodness of fit is determined by comparing the FITEQL calculated variance function value, $V(Y)$, for each data set, and the model that yields the lowest $V(Y)$ value represents the best fit. Fig. 2B shows a representative example of a model developed using the four site model and its fit to the titration data for one consortium (dashed curve). For each of the 53 titrations, a four site model provides an excellent fit to the observed buffering behavior.

All titration modeling results are compiled in Table 1, and the table also shows averages for all of the river water, forest soil, and soybean field soil samples separately. There are no significant trends in the pK_a values for any of the four sites, or for their site concentrations, as functions of either sampling site or time of year. Therefore, we conclude that bacterial diversity does not affect proton uptake significantly for the species represented in the consortia of this study, and a single set of averaged pK_a values and site concentrations can be used to account for the observed proton uptake by all of the consortia. The pK_a and site concentration values that are averaged over the entire dataset are also compiled in Table 1. The functional group sites with pK_a values of 3.2, 4.8, 6.5, and

9.2 are hereafter referred to as sites A_1 through A_4 , respectively (Table 1). Fig. 2B illustrates that the averaged pK_a values and surface site concentrations yield a virtually identical fit (solid curve in the figure) to the representative titration data to that offered by the best-fit model of that data. The averaged pK_a values are similar to those calculated by Borrok et al. (2004a,b) for both the natural consortia from contaminated and uncontaminated environments.

Site densities for each of the four discrete sites are similar for all consortia and the average total site concentrations (the sum of the average concentrations of binding sites for each of the four surface sites) range from 3.7×10^{-4} to 3.9×10^{-4} mol of sites per gram of consortium. Titration data alone cannot be used to determine the identity of the individual functional group types present on the cell walls. However, it is interesting to note that the buffering capacities of the large number of complex mixtures of bacterial species studied here can be modeled well using the same set of averaged acidity constants and site concentrations. It is possible that the commonality in these parameters represents a commonality in binding site types among these bacterial species, but a rigorous testing of this hypothesis must await further spectroscopic study.

The uncertainties determined for the averaged acidity constants reported in Table 1 represent a range of 1 σ standard deviation in the non-logarithmic values. For Sites A_1 – A_3 , especially, the magnitude of these uncertainties is strongly affected by only a few very high calculated K_a values (Fig. 5). For example, the calculated K_a values from Titration 14 are 8.2, 3.3, and 5.6 times greater than the averaged K_a values for Sites A_1 – A_3 , respectively. Most of the calculated K_a values exhibit a significantly lower degree of variability than is implied by the calculated standard deviations. It is unclear whether these few high calculated K_a values arise due to experimental uncertainties or from real variability in K_a values, so we include all values in our calculated averages. Even with the higher calculated K_a values included, the uncertainty values associated with the averages are of similar magnitude to those reported by previous studies for K_a values for single species of bacteria (e.g. Fein et al., 1997; Haas et al., 2001; Martinez et al., 2002; Ngwenya et al., 2003; Fein et al., 2005). The uncertainties associated with the averaged values from this study suggest that the degree of observed variability for the range of consortia studied arises more from experimental uncertainties than from real differences in the buffering capacities of the different consortia. The calculated surface site concentrations from this study (Table 1) are significantly higher than those determined by Borrok et al. (2004a) for similar bacterial consortia,

Table 1
Calculated proton binding constants (pK_a) and surface site concentrations

Consortia		Proton binding constants ($-\log K_a$)				Site concentrations ($\times 10^{-5}$ mol/g w.w.)				
		A ₁	A ₂	A ₃	A ₄	A ₁	A ₂	A ₃	A ₄	T ^a
River	Oct.	3.5	4.8	6.6	9.2	7.6	10.8	6.8	9.9	1
		3.8	5.1	6.8	9.2	6.7	8.2	6.1	11.0	2
	Nov.	3.7	5.1	7.0	9.2	6.7	8.1	7.0	11.2	3
		3.7	5.1	7.2	9.5	6.2	7.6	10.0	14.2	4
		3.6	5.1	6.9	9.4	9.2	10.9	5.5	9.8	5
		3.6	4.9	6.6	9.2	8.7	10.6	6.4	9.7	6
		3.7	5.1	6.9	9.3	9.3	10.6	5.3	9.9	7
	March	3.0	4.7	6.6	9.3	12.3	14.5	6.6	9.6	8
		2.8	4.7	6.5	9.2	17.1	21.0	9.3	14.4	9
		3.5	4.9	6.6	9.1	8.4	10.6	4.9	7.9	10
	May	3.4	4.8	6.5	8.9	7.3	10.1	4.8	8.2	11
		3.5	4.8	6.9	9.2	7.7	11.0	4.6	9.4	12
	June	2.5	4.6	6.1	9.0	18.1	13.1	7.1	7.7	13
		2.2	4.3	5.8	8.8	22.0	11.2	8.1	6.6	14
		3.1	4.7	6.4	9.0	11.4	12.6	7.0	7.6	15
	Sept.	2.7	4.4	6.1	8.9	12.7	12.1	8.1	7.0	16
		3.1	4.8	6.4	9.1	11.5	12.1	6.7	7.6	17
Forest	Oct.	3.6	4.9	6.7	9.2	9.9	10.5	5.5	10.1	18
		3.4	4.9	6.6	9.2	11.4	11.8	6.7	9.2	19
	Nov.	3.6	4.9	6.7	9.3	11.1	11.6	6.0	11.7	20
		3.2	4.6	6.5	9.2	9.7	13.5	7.4	12.3	21
		3.7	5.1	7.1	9.5	10.1	13.3	5.1	14.4	22
		3.5	5.0	6.9	9.3	8.2	12.0	4.8	11.7	23
		3.5	4.8	6.6	9.2	7.7	13.3	5.7	13.7	24
	March	3.4	4.8	6.6	9.3	12.2	14.0	6.3	11.0	25
		3.2	4.7	6.5	9.2	10.0	14.8	6.3	11.0	26
		3.3	4.7	6.5	9.1	8.8	12.3	5.7	8.2	27
	May	3.5	4.8	6.7	9.2	8.1	11.0	5.2	9.1	28
		3.4	4.8	6.1	9.2	8.0	1.0	5.0	8.0	29
	June	3.1	4.7	6.6	9.2	11.5	13.2	6.4	8.6	30
		3.1	4.7	6.6	9.2	11.3	12.8	6.2	8.4	31
		3.1	4.7	6.5	9.2	11.9	14.0	6.4	9.3	32
	Sept.	3.1	4.6	6.2	9.1	10.2	15.2	6.7	1.1	33
		3.2	4.7	6.6	9.2	11.4	18.8	5.1	1.3	34
Crop	Oct.	3.5	4.9	6.8	9.3	8.8	13.4	4.7	11.2	35
		3.4	4.9	6.7	9.1	9.6	10.8	6.2	8.4	36
	Nov.	3.6	5.0	6.8	9.2	8.6	9.3	5.5	8.4	37
		3.5	5.0	6.7	9.3	8.5	9.4	5.8	9.3	38
		3.4	4.9	6.8	9.3	10.2	13.0	5.6	8.3	39
		3.5	4.9	6.7	9.2	10.3	13.9	6.1	9.2	40
		3.6	5.0	6.7	9.3	9.7	12.1	5.5	11.6	41
	March	3.2	4.8	6.7	9.3	11.3	13.5	5.7	7.7	42
		3.3	4.8	6.7	9.3	10.7	13.9	5.4	9.5	43
		3.4	4.8	6.7	9.3	9.7	13.2	5.4	9.9	44
	May	3.4	4.9	6.7	9.2	10.1	13.6	5.5	9.3	45
		3.4	4.8	6.7	9.1	8.8	12.8	5.2	8.1	46
	June	3.5	4.9	6.7	9.3	9.0	11.8	5.4	9.4	47
		2.9	4.7	6.5	9.3	13.2	13.3	6.7	8.0	48
		2.7	4.6	6.3	8.9	13.7	12.4	6.9	6.3	49
	Sept.	2.9	4.7	6.4	9.1	11.7	11.5	6.2	6.0	50
		3.2	4.8	6.6	9.2	11.1	12.0	5.5	8.0	51
3.2		4.7	6.6	9.3	10.2	13.2	5.8	9.8	52	
		3.3	4.8	6.6	9.3	9.8	12.4	6.0	11.8	53

(continued on next page)

Table 1 (continued)

Consortia	Proton binding constants ($-\log K_a$)				Site concentrations ($\times 10^{-5}$ mol/g w.w.)				
	A ₁	A ₂	A ₃	A ₄	A ₁	A ₂	A ₃	A ₄	T ^a
<i>Averages^{b,c}</i>									
River	2.97	4.73	6.43	9.18	10.8	11.5	6.7	9.5	
Forest	3.3	4.77	6.59	9.21	10.0	13.1	5.9	10.6	
Crop	3.23	4.81	6.64	9.22	10.3	12.4	5.7	9.0	
Overall	3.15	4.77	6.54	9.18	10.4	12.4	6.1	9.7	
Stdev ^{d,e}	+0.2/-0.38	+0.16/-0.27	+0.26/-0.76	+0.07/-0.25	±2.78	±2.28	±1.07	±2.04	

^aTitration number, refers to numbers plotted in Fig. 5.

^bThe binding constants reported are an average calculated from the individual (non-log) equilibrium constants for the specific site for the consortia of interest.

^cOverall averages are an average calculated from the individual (non-log) equilibrium constants. These values are utilized for metal adsorption models.

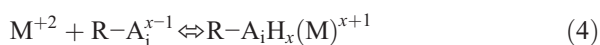
^dBecause of outlier values, the standard deviation is larger than the average and can not be reported in log form. Therefore, we neglect the K values greater than 1.5×10^{-3} in calculating the standard deviation for A₁.

^eReported uncertainties were calculated using the following formulas: +uncertainty = $\log(\text{Ave} + \text{stdev}) - \log(\text{Ave})$, -uncertainty = $\log(\text{Ave}) - \log(\text{Ave} - \text{stdev})$ where Ave represents the average, site-specific equilibrium constant calculated from all experimental data. Stdev represents the standard deviation of the average.

possibly due to differences in bacterial growth conditions and growth media between the two studies.

In general, the similarity in titration curves among all of the consortia studied here, and the associated low degree of uncertainty in the averaged acidity constants and site concentrations, demonstrates that one set of averaged acidity constants and surface site concentrations is adequate to reasonably describe the proton adsorption behavior of all of the natural consortia in this study. These similarities imply a commonality of binding sites among the various bacterial cell wall functional groups present in all of the consortia in this study, and suggest that the averaged acidity constants and site concentrations may be used to provide a reasonable model for proton adsorption, buffering capacity, and surface charge for bacterial consortia in a wide range of natural systems.

Following the approach of Borrok et al. (2004a), we use FITEQL 2.0, along with the average acidity constant and site concentration values determined from the titration models, to account for cation (M^{+2}) adsorption onto the cell wall according to the reaction:



where $R-A_iH_x(M)^{x+1}$ represents the metal–bacterial surface complex. The mass balance equation for reaction X is:

$$K_{\text{ads}} = \frac{[R-AH_x(M)^{x+1}]}{a_{M^{+2}} [R-AH_x^{x-1}]} \quad (5)$$

where the brackets represent concentration in moles of sites L^{-1} , a represents the activity of the subscripted species, and K_{ads} is the thermodynamic equilibrium constant for reaction 4. A 1:1 metal:surface site stoichiometry was used in all models. These calculations account for aqueous metal hydrolysis reactions using equilibrium constants from Baes and Mesmer (1976), and they use the water dissociation constant from Wolery (1992). Metal adsorption measurements conducted as a function of pH were used to determine the minimum number of binding sites and the best fit metal–bacterial adsorption stability constants (Tables 2 and 3).

The number of sites required to adequately describe cation adsorption varies, depending mostly on the pH range of the data and the extent of metal adsorption observed for a specific metal. We only considered models in which the metal adsorbs onto a single site or onto sites with sequential pK_a values (i.e., adsorption to sites A₁ and A₂ or onto A₁, A₂, and A₃). In cases in which the pH range of the data was limited, only a 2 or 3-site model was required to fit the experimental data. In all cases, when adsorption data were collected at pH values higher than 8, a fourth site was required to account for the adsorption at high pH. The best-fit model for each consortium and the average stability constant value for each site are tabulated in Table 2. The metal stability constants for A₄ could be better constrained with more experiments at high pH with varying metal:bacteria ratios. Other than for the A₄ site, the uncertainties for the averaged metal–bacterial stability constants are of similar magnitude to those reported by previous studies for single species of bacteria (e.g., Fowle and Fein, 1999; Haas et al.,

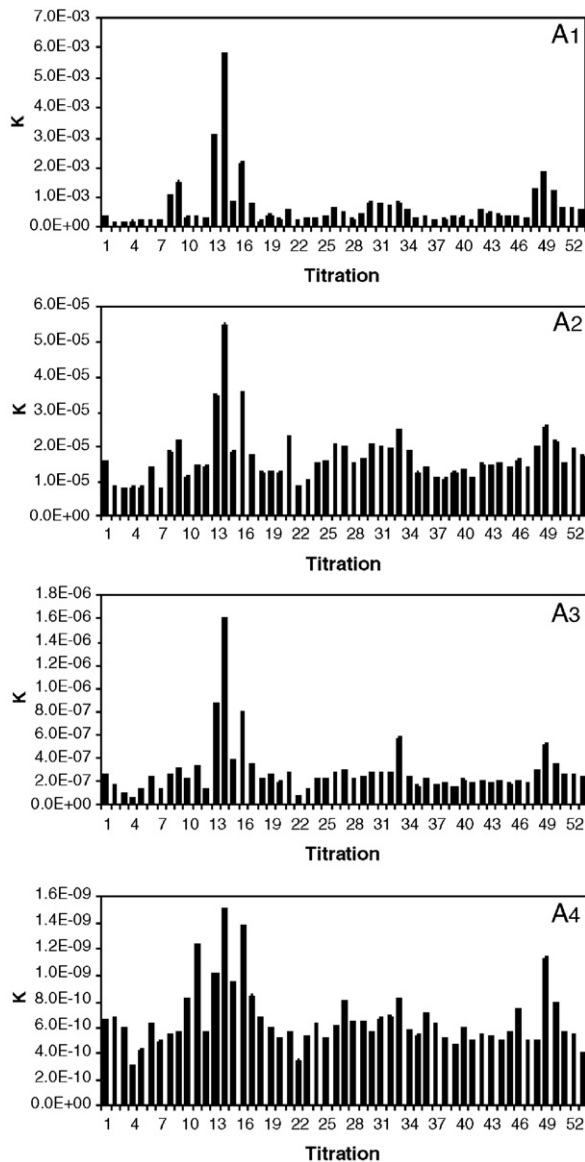


Fig. 5. Histogram of calculated acidity constant values for each titration. The titration numbers correspond to the values listed in Table 1.

2001; Yee and Fein, 2001; Ngwenya et al., 2003), providing evidence that the variability in metal adsorption behavior is largely due to experimental uncertainty rather than to real differences in the adsorption capacities of individual bacterial species.

An averaged four-site adsorption model, constructed using the averaged acidity constants, site concentrations, and the averaged Cd-consortia stability constants given in Tables 1 and 2, yields a reasonable fit to the observed Cd adsorption behavior (Fig. 3). The model fit lies within 20% of the observed adsorption percentages in all cases, and for much of the pH range the fit is within

Table 2
Cd binding constants ($\log K$) for best-fit adsorption models

Consortia		Cd binding constants ($\log K$)			
		A ₁	A ₂	A ₃	A ₄
River	Oct.	3.1	3.4		
	Nov.	3.0	2.9	2.8	6.0
	Jan.	3.4	3.0	4.2	5.8
	March		3.6	4.3	
	May	2.5	3.0	4.2	
	June	2.9	2.9	4.0	5.0
Forest	Sept.	2.9	3.0	4.1	
	Oct.	3.3	3.4	3.9	6.3
	Nov.	3.2	3.4	4.3	5.5
	Jan.	3.4	3.4	4.5	
	March	2.7	3.3	4.2	
	May	3.1	3.5	4.2	
Soybean	June	3.0	3.5	4.5	5.5
	Sept.	2.9	3.6	3.6	5.8
	Oct.	3.5	3.3	4.7	
	Nov.	3.1	3.2	4.1	5.6
	Jan.	2.9	3.6	3.5	5.8
	March	3.0	3.4	4.3	
Averages ^{a,b}	May	3.1	3.4	4.3	4.7
	June	3.2	3.3	4.6	
	Sept.	2.8	3.6	4.2	5.6
	Water	3.0	3.2	4.1	5.8
	Corn	3.1	3.4	4.4	5.6
	Forest	3.2	3.5	4.3	5.9
Total	3.1	3.4	4.3	5.8	
Stdev		+0.20/ -0.38	+0.18/ -0.29	+0.23/ -0.50	+0.28/ -0.94

^aThe metal stability constants reported represent an average calculated from the individual (non-log) equilibrium constants for the specific site and consortia of interest.

^bUncertainties were calculated using the following formulas: +uncertainty = $\log(\text{Ave} + \text{stdev}) - \log(\text{Ave})$, -uncertainty = $\log(\text{Ave}) - \log(\text{Ave} - \text{stdev})$ where Ave represents the average, site-specific metal stability constant calculated from all experimental data. Stdev represents the standard deviation of the average.

10% of the extremes in adsorption that we observed. At high pH (8.5 and above), the averaged model over-predicts the extent of adsorption by up to 5–10%, suggesting that the Cd-A₄ binding environment is not

Table 3
Metal binding constants ($\log K$) for best-fit adsorption models

Metal	Metal binding constants ($\log K$)			
	A ₁	A ₂	A ₃	A ₄
Ca	1.8	2.3	2.9	
Cu	3.8	3.9	5.5	
Pb			7.1	
Sr	2.5	1.9	3.1	
Zn	2.6	2.8	3.5	5.7

well-described by the model. The best-fitting three-site model (also depicted in Fig. 3) yields a bigger misfit to the observed adsorption under high pH conditions, clear evidence that a fourth binding site must be involved in the uptake of Cd at these pH values. There is considerably more uncertainty associated with the model fit to the Cd adsorption data for the consortia studied here than is typically associated with model fits to metal adsorption onto single bacterial species. However, the level of uncertainty is acceptably small for field applications of this modeling approach where it is likely that the uncertainties associated with using these averaged parameters to model Cd adsorption are relatively small compared to the uncertainties in determining bacterial concentrations in realistic settings.

A similar modeling approach was applied to account for the adsorption of the other metals studied here onto the river water consortia, and the results are compiled in Table 3 and depicted in Fig. 4. The number of surface sites required to account for the adsorption of Ca, Cu, Pb, Sr, and Zn depends on the pH range of the adsorption data as well as on the extent of adsorption for each metal. In general, the best-fit models account for the data well, with the Pb and Zn models displaying the best fits. The stability constants obtained for the metals studied here were similar in magnitude to those obtained previously for single species of bacteria (Fowle and Fein, 1999; Fein et al., 2001; Ngwenya et al., 2003; Yee and Fein, 2003; Borrok and Fein, 2005).

The Cd experiments rigorously tested the hypothesis of universal binding mechanisms using a wide range of bacterial consortia. Given the similarities in binding that we observed, the primary purpose for conducting the Ca, Cu, Pb, Sr, and Zn experiments was not to repeat tests on a diverse collection of consortia, but to calibrate a linear free-energy approach (Langmuir, 1979) for estimating metal-consortia stability constants for metals not studied here. In this approach, we relate the stability constants for the metal–bacterial surface complexes that are calculated in this study to the stability constants for acetate complexes involving these same metals. This approach yields good correlations for single bacterial species, such as *Bacillus subtilis* (Fein et al., 1997; Fein et al., 2001). Other than the Pb data which were fit with a Site A₃-only model, all model fits included metal binding onto the A₂ site (4.77 pK_a) and the A₃ site (6.54 pK_a). We relate the metal–A₂ and metal–A₃ stability constants to the corresponding metal–acetate stability constants from Shock and Koretsky (1993), with the results depicted in Fig. 6. There is a reasonable relationship in each case, with metal–bacterial stability constants increasing in general with increasing metal–

acetate stability constant value. We fit the data with linear relationships, with correlation coefficients of 0.95 and 0.92, respectively, for the Site A₂ and Site A₃ relationships. These correlations likely result from similarities in binding environments between acetate and the A₂ and A₃ sites on the bacterial consortia. The equations of the best-fitting lines shown in Fig. 6A and B are

$$Y = (1.37)*X + 0.70 \quad (6)$$

$$Y = (2.53)*X + 0.05 \quad (7)$$

where X and Y represent the logarithm of the stability constant values for the metal–acetate and metal–A₂ or metal–A₃ complexes, respectively. These relationships can be used to estimate metal–A₂ and metal–A₃ stability constants for bacterial consortia, if the stability constant for the corresponding metal–acetate complex is known. Therefore, these types of relationships are important for extrapolating these experimental and modeling results to estimate the extent of adsorption that would occur between bacterial consortia and metals not studied here.

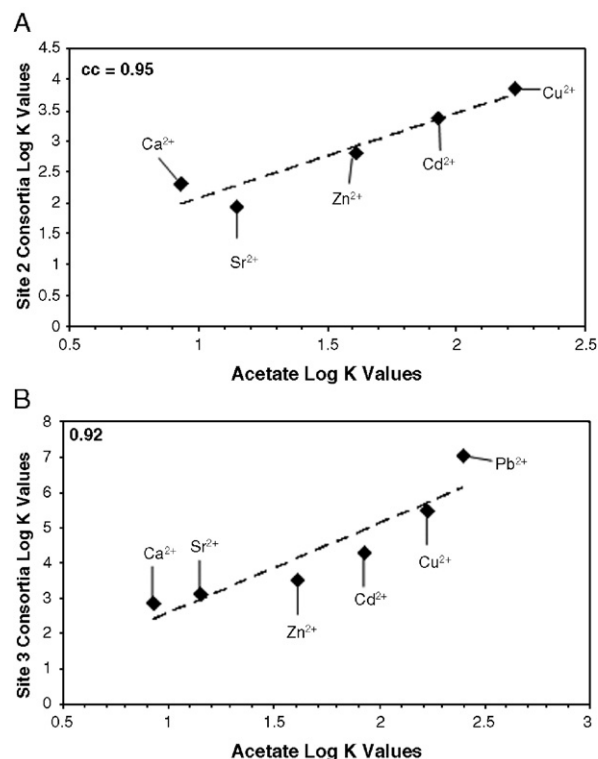


Fig. 6. Correlation plots showing metal–bacterial stability constants calculated from experiments using the bacterial consortia and corresponding metal–acetate stability constants from Shock and Koretsky (1993). Linear correlation coefficients are shown for each data set.

4. Conclusions

In this study, we used adsorption experiments onto bacterial consortia grown from a range of environments collected over the course of a year to extensively test if commonalities exist in the adsorption behavior of protons and Cd. We observed nearly identical proton adsorption behavior and similar Cd adsorption behavior for all of the consortia tested, and we quantify the acidity constants, site concentrations, and stability constants for the important metal–bacterial surface complexes. The uncertainties associated with the averaged acidity constants, site concentrations, and stability constant values from all of the consortia datasets are similar in magnitude to those associated with acidity constants, site concentrations, and stability constant values from adsorption experiments that involved single bacterial species. Therefore, the variability that is seen in the adsorption behaviors in this study likely results primarily from experimental uncertainty and not from real trends in binding behavior as a function of bacterial diversity. The consortia that we used in the adsorption experiments represent a wide range in bacterial diversity. Therefore, although there clearly are some bacteria in nature that exhibit different adsorption behaviors (e.g., Borrok et al., 2004b), it is likely that the common adsorption behavior documented here holds for an even wider range of bacteria than was tested in this study.

The Cd experiments demonstrate the universality of metal adsorption behavior onto a wide range of bacterial consortia. Based on these results, we measured the adsorption of Ca, Cu, Pb, Sr, and Zn onto individual consortia in order to calibrate a linear free energy approach that enables predictions of the adsorption behavior of other metals onto bacterial consortia. Therefore, this study yields a set of averaged acidity constants, surface site concentrations, and metal stability constants that can be used to estimate metal speciation and adsorption in realistic bacteria-bearing systems. The usefulness of this averaged model depends on the particular application of interest. In engineered systems, it may be useful and possible to determine the extent of bacterial metal adsorption with greater precision than this averaged model provides. However, in complex geologic systems, it is impossible to study the adsorption properties of each metal and each bacterial species of interest. Therefore, this generalized model, with its slightly higher level of uncertainty, offers a useful approach for quantifying the fate and transport of metals.

Acknowledgements

This research was sponsored by a National Science Foundation Environmental Molecular Science Institute grant to University of Notre Dame (EAR-0221966). Two journal reviews and the comments of Chief Editor David Rickard significantly improved the presentation of the manuscript.

References

- Baes, C.F., Mesmer, R.E., 1976. *The Hydrolysis of Cations*. Wiley, New York, USA.
- Beveridge, T.J., Koval, S.F., 1981. Binding of metals to cell envelopes of *Escherichia coli*-K-12. *Appl. Environ. Microbiol.* 42, 325–335.
- Beveridge, T.J., Murray, R.G.E., 1976. Uptake and retention of metals by cell walls of *Bacillus subtilis*. *J. Bacteriol.* 127, 1502–1518.
- Borrok, D., Fein, J.B., 2005. The impact of ionic strength on the adsorption of protons, Pb, Cd, and Sr onto the surfaces of Gram negative bacteria: testing non-electrostatic, diffuse, and triple-layer models. *J. Colloid Interface Sci.* 286, 110–126.
- Borrok, D., Fein, J.B., Kulpa, C.F., 2004a. Proton and Cd adsorption onto natural bacterial consortia: testing universal adsorption behavior. *Geochim. Cosmochim. Acta* 68, 3231–3238.
- Borrok, D., Fein, J.B., Kulpa, C.F., 2004b. Cd and proton adsorption onto bacterial consortia grown from industrial wastes and contaminated geologic settings. *Environ. Sci. Technol.* 38, 5656–5664.
- Borrok, D., Fein, J.B., Turner, B.F., 2005. A universal surface complexation framework for modeling proton binding onto bacterial surfaces in geologic settings. *Am. J. Sci.* 305, 826–853.
- Daughney, C.J., Fein, J.B., Yee, N., 1998. A comparison of the thermodynamics of metal adsorption onto two common bacteria. *Chem. Geol.* 144, 161–176.
- Fein, J.B., Daughney, C.J., Yee, N., Davis, T.A., 1997. A chemical equilibrium model for metal adsorption onto bacterial surfaces. *Geochim. Cosmochim. Acta* 61, 3319–3328.
- Fein, J.B., Martin, A.M., Wightman, P.G., 2001. Metal adsorption onto bacterial surfaces: development of a predictive approach. *Geochim. Cosmochim. Acta* 65, 4267–4273.
- Fein, J.B., Boily, J.-F., Yee, N., Gorman-Lewis, D., Turner, B.F., 2005. Potentiometric titrations of *Bacillus subtilis* cells to low pH and a comparison of modeling approaches. *Geochim. Cosmochim. Acta* 69, 1123–1132.
- Fowle, D.A., Fein, J.B., 1999. Competitive adsorption of metal cations onto two gram positive bacteria: testing the chemical equilibrium model. *Geochim. Cosmochim. Acta* 63, 3059–3067.
- Haas, J.R., Dichristina, T.J., Wade Jr., R., 2001. Thermodynamics of U(VI) sorption onto *Shewanella putrefaciens*. *Chem. Geol.* 180, 33–54.
- Jiang, W., Saxena, A., Song, B., Ward, B.B., Beveridge, T.J., Myneni, S.C.B., 2004. Elucidation of functional groups on Gram-positive and Gram-negative bacterial surfaces using infrared spectroscopy. *Langmuir* 20, 11433–11442.
- Kaerberlein, T., Lewis, K., Epstein, S.S., 2002. Isolating “uncultivable” microorganisms in pure culture in a simulated natural environment. *Science* 296, 1127–1129.
- Kulczycki, E., Ferris, F.G., Fortin, D., 2002. Impact of cell wall structure on the behavior of bacterial cells as sorbents of cadmium and lead. *Geomicrobiol. J.* 19, 553–565.

- Langmuir, D., 1979. Techniques of estimating thermodynamic properties for some aqueous complexes of geochemical interest. In: Jenne, E.A. (Ed.), *Chemical Modeling in Aqueous Systems*. American Chemical Society, pp. 357–387.
- Martinez, R.E., Smith, D.S., Kulczycki, E., Ferris, F.G., 2002. Determination of intrinsic bacterial surface acidity constants using a Donnan shell model and a continuous pK_a distribution method. *J. Colloid Interface Sci.* 253, 130–139.
- Mullen, M.D., Wolf, D.C., Ferris, F.G., Beveridge, T.J., Flemming, C.A., Baily, G.W., 1989. Bacterial sorption of heavy metals. *Appl. Environ. Microbiol.* 55, 3143–3149.
- Muyzer, G., De Waal, E.C., Uitterlinden, A.G., 1993. Profiling of complex microbial populations by denaturing gradient gel electrophoresis analysis of polymerase chain reaction-amplified genes coding for 16S rRNA. *Appl. Environ. Microbiol.* 59, 695–700.
- Ngwenya, B.T., Sutherland, I.W., Kennedy, L., 2003. Comparison of the acid–base behaviour and metal adsorption characteristics of a gram-negative bacterium and other strains. *Appl. Geochem.* 18, 527–538.
- Plette, A.C.C., van Riemsdijk, W.H., Benedetti, M.F., Van der Wal, A., 1995. pH dependent charging behavior of isolated cell walls of a gram-positive soil bacterium. *J. Colloid. Interface Sci.* 173, 354–363.
- Plette, A.C.C., Benedetti, M.F., Van Riemsdijk, W.H., 1996. Competitive binding of protons, calcium, cadmium, and zinc to isolated cell walls of a Gram-positive soil bacterium. *Environ. Sci. Technol.* 30, 1902–1910.
- Sambrook, J., Fritsch, E.F., Maniatis, T., 1989. 2nd ed. *Molecular Cloning, a Laboratory Manual*, vol. 3. Cold Spring Harbor Laboratory Press, New York.
- Shock, E.L., Koretsky, C.M., 1993. Metal–organic complexes in geochemical processes: Calculation of standard partial molal thermodynamic properties of aqueous complexes at high pressures and temperatures. *Geochim. Cosmochim. Acta* 57, 4899–4922.
- Small, T.D., Warren, L.A., Rodden, E.E., Ferris, F.G., 1999. Sorption of strontium by bacteria, Fe(III) oxide, and bacteria–Fe(II) oxide composites. *Environ. Sci. Technol.* 33, 4465–4470.
- Westall, J.C., 1982. FITEQL, a Computer Program for Determination for Chemical Equilibrium Constants from Experimental Data. Version 2.0. Oregon St. University, Corvallis, OR.
- Westall, J.C., Jones, J.D., Turner, G.D., Zachara, J.M., 1995. Models for association of metal ions with heterogeneous environmental sorbents. 1. Complexation of Co(II) by leonardite humic acid as a function of pH and NaClO₄ concentration. *Environ. Sci. Technol.* 29, 951–959.
- Wolery, T.J., 1992. EQ4NR, a Computer Program for Geochemical Aqueous Speciation-Solubility Calculations: Theoretical Manual, User's Guide, and Related Documentation (Version 7.0). UCRL-MA-110662-PT-III. Lawrence Livermore Natl. Lab., Livermore, CA, USA.
- Yee, N., Fein, J.B., 2001. Cd adsorption onto bacterial surfaces: a universal adsorption edge? *Geochim. Cosmochim. Acta* 65, 2037–2042.
- Yee, N., Fein, J.B., 2003. Quantifying metal adsorption onto bacteria mixtures: a test and application of the surface complexation model. *Geomicrobiol. J.* 20, 43–60.